Near-field imaging of coupled photonic-crystal microcavities

Silvia Vignolini,[1] Francesca Intonti,[2,a)] Margherita Zani,[2] Francesco Riboli,[1]
Diederik S. Wiersma,[1] Lianhe H. Li,[3] Laurent Balet,[3] Marco Francardi,[4]
Annamaria Gerardino,[4] Andrea Fiore,[5] and Massimo Gurioli[2]

[1]*LENS and INFM-BEC, Via Nello Carrara 1, 50019 Sesto Fiorentino, Italy*
[2]*CNISM, Department of Physics and LENS, University of Florence, Via Nello Carrara 1, 50019 Sesto Fiorentino, Italy*
[3]*EPFL, Institute of Photonics and Quantum Electronics, Station 3, CH-1015 Lausanne, Switzerland*
[4]*Institute of Photonics and Nanotechnology, CNR, via del Cineto Romano 42, 00156 Roma, Italy*
[5]*COBRA Research Institute, Eindhoven University of Technology, 5600 MB Eindhoven, The Netherlands*

We report by means of near-field microscopy on the coupling between two adjacent photonic crystal microcavities. Clear-cut experimental evidence of the spatial delocalization of coupled-cavity optical modes is obtained by imaging the electromagnetic local density of states. We also demonstrate that it is possible to design photonic structures with selective coupling between different modes having orthogonal spatial extensions © *2009 American Institute of Physics.*
[DOI: 10.1063/1.3107269]

Coupling between two spatially separated photonic crystal micro-cavity (PC-MC) modes has been recently proposed for application in quantum information and communication.[1,2] The cavity coupling of microresonators has been demonstrated in different systems such as microdisks,[3] pillar cavities,[4,5] and in PC-MCs,[6] and recently the idea has been used for applications in photonic devices such as lasers,[7] optical waveguides,[8] and memories.[9] Similar to the case of electronic states, in the ideal case of identical cavities and under the main prerequisites of frequency matching and spatial overlap, the coupling results in an energy splitting of the modes and in the formation of delocalized "symmetric" and "antisymmetric" coupled modes. However, in real samples the presence of a double peak in the spectrum can be the signature either of cavity coupling or of fabrication induced dielectric disorder. In order to investigate the cavity coupling conditions, one has to add information about the spatial distribution of the electric field. Coupled-cavity modes are delocalized over the two cavities, while in the uncoupled situation the field distribution results localized to either one of the two cavities.

In this letter, we study the coupling of PC-MCs by means of scanning near field microscopy (SNOM), whose resolution is well below both the diffraction limit and the mode spatial extension.[10–13] It has been recently shown that the near-field tip induced spectral shift map gives a direct and high fidelity mapping of the electromagnetic local density of states (LDOS).[14] By imaging the LDOS we obtain clear-cut experimental evidences either of the spatial delocalization of modes over the two coupled PC-MCs or of the localization of the modes on a single PC-MCs in the case of large frequency mismatch.

We use a GaAs based heterostructure: three layers of high-density InAs QDs emitting at 1300 nm are grown by molecular beam epitaxy at the center of a 320-nm-thick GaAs membrane.[15] The structure under consideration consists of a two-dimensional triangular lattice of air holes with lattice parameter $a=311$ nm and filling fraction $f=35\%$,

where the cavity is formed by four missing holes organized in a diamond-like geometry (denominated D2 cavity, see inset (l) in Fig. 1 where the topographic map is reported). Here we study both spectrally and spatially the coupling regime
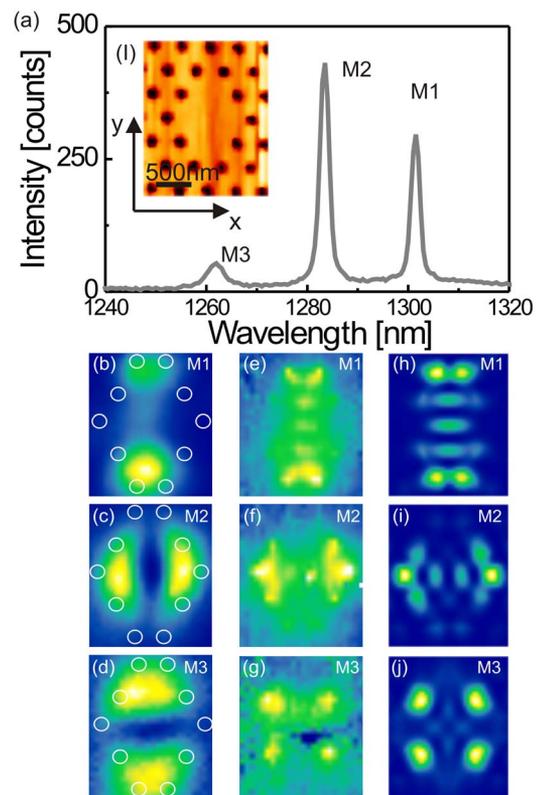

FIG. 1. (Color online) (a) Near-field spectrum of the single D2 PC-MC (averaged on a region of 2×2 μm^2). [(b)–(d)] PL intensity maps associated to the M1-M3 modes; the holes surrounding the D2 defect are reported as white circles. [(e)–(g)] Spectral shift maps associated to the M1-M3 modes; in particular the maximum spectral shift in (e) and (f) is 0.2 nm, while in (g) is 0.5 nm. [(h)–(j)] Calculated electric field distribution of the M1-M3 modes at 30 nm above the photonic membrane. (i) Topographic map as obtained during the SNOM scan. All the maps in (b)–(j) have the same spatial extension (1.3×1.6 μm^2).

a)Electronic mail: intonti@lens.unifi.it.

94, 151103-1

for two different coupled systems. Henceforth we will refer to vertically (horizontally) aligned D2 cavities if the major (minor) diagonals of the two adjacent D2 cavities lie along the same line. In both cases the coupled cavities have a single-hole barrier. A room temperature commercial SNOM (Twinsnom, OMICRON) is used in an illumination-collection geometry. The sample is excited with light from a diode laser (780 nm) coupled into a chemically etched optical fiber, which allows us to have a direct measurement of the LDOS through the spectral shift map.[14] Photoluminescence (PL) spectra from the sample were collected at each tip position through the same probe and the PL signal dispersed by a spectrometer was detected by a liquid nitrogen cooled InGaAs array with a low (high) spectral resolution of 1 nm (0.1 nm). Numerical calculations were performed with a commercial three-dimensional finite-difference time domain code (CrystalWave, Photond). The calculations are performed using the nominal parameters of the structure, not including the effects of fabrication-induced disorder, with a refractive index of 3.48 and a grid of 25 nm. As excitation sources we employed randomly placed dipoles with different orientations.

In order to better understand the effects of the coupling, the main properties of a single D2 cavity are summarized in Fig. 1. Figure 1(a) reports the spectrum and, in inset (l), the topographic map and a (x,y) reference system in the PC-MC plane with the vertical y (horizontal x) axis aligned to the principal (secondary) diagonals of the D2 cavity. Three peaks are observed in the spectrum, corresponding to three PC-MC modes (labeled M1, M2, and M3). For each mode we report three spatial distributions: the PL intensity maps [Figs. 1(b)–1(d)], the tip induced spectral shift maps [Figs. 1(e)–1(g)], and the simulated LDOS maps [Figs. 1(h)–1(j)] associated to each peak. The spectral shift reproduce the LDOS with much better fidelity than the PL intensity maps,[14] as clearly shown in Fig. 1. Note that the spatial resolution in the determination of the LDOS (measured by the full width at half maximum of the more confined lobe in the experimental spectral shift map) is of the order of 80 nm (corresponding to the quite striking value of $\lambda/16$). The M1 mode is elongated along the y direction, the M2 mode is prevalently elongated along the x direction, while the M3 mode is mainly distributed at the vertexes of a square. In the following discussion of the two coupled D2 cavities, we will concentrate only on the M1 and M2 modes.

The coupled-cavity system can be generally described by two linearly coupled oscillators (the modes of each isolated cavity in our case) obtaining the formula of the photonic splitting for coupled-cavity modes $\Omega = \sqrt{\Delta^2 + 4g^2}$ (where Δ is the disorder induced energy detuning and g is the coupling energy of the modes of each isolated cavity).[6] Only for $\Delta = 0$ that the photonic splitting Ω is a direct measurement of the coupling energy g; in the case $\Delta \gg g$ the system is uncoupled and $\Omega \approx \Delta$. In our case, the M1 and M2 modes of the D2 cavity have very distinct LDOS and are expected to show different coupling constants g in the horizontal and vertical coupling design.

In Fig. 2 the experimental results for horizontally (along x) coupled PC-MCs are compared with the calculated electric field intensity. The PL maps indicate that P1 and P2 are localized on a single cavity, and more precisely the PL signal associated to P1 is concentrated on the left cavity [Fig. 2(b)],
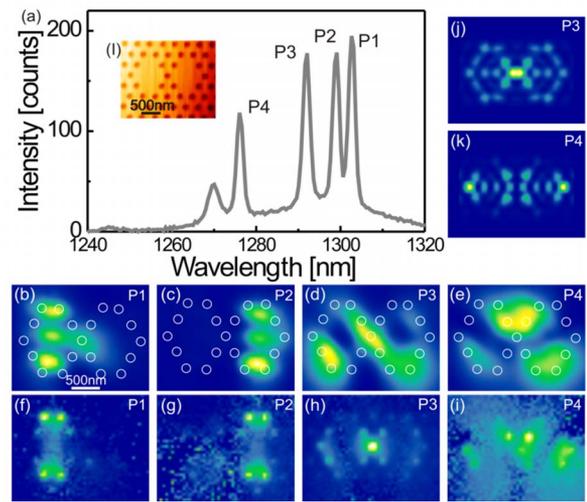

FIG. 2. (Color online) (a) Near-field spectrum of the horizontally coupled D2 PC-MCs (averaged on a region of 2×3 μm^2). Inset (i): topographic map as obtained during the SNOM scan. [(b)–(e)] PL intensity maps associated to the peak P1-P4. [(f)–(i)] Spectral shift maps associated to the peak P1-P4; in particular the maximum spectral shift in (f) and (g) is 0.3 nm, in (h) is 0.5 nm, and in (i) is 0.2 nm. [(j) and (k)] Calculated electric field distribution of P3 and P4 at 30 nm above the photonic membrane. All the maps have the same spatial extension (2.4×2.0 μm^2).

while the PL signal associated to P2 is concentrated on the right cavity [Fig. 2(c)]. On the contrary the PL signal related to P3 and P4 is delocalized on the entire system [Figs. 2(d) and 2(e)]. The spectral shift maps permit to gain more insights into the nature of the different modes and to correlate them with the modes of a single D2 cavity. Both P1 and P2 resemble very closely the M1 mode of a single D2 cavity [Fig. 1(e)], demonstrating that the coupling energy g for the M1 modes of the two horizontally aligned D2 cavities is very small, if any. This means that the spectral splitting of 2.6 meV between P1 and P2 has to be ascribed to the energy detuning Δ due to structural disorder in the cavity realization. A different situation occurs for P3 and P4 resonances. Their spectral shift maps strongly suggest that P3 and P4 are the two coupled-cavity modes originating from the M2 modes of the two D2 cavities. This is clearly demonstrated by the comparison of the experimental data for P3 [Fig. 2(h)] with the corresponding simulated map of the LDOS, as reported in Fig. 2(j). The spatial distribution of both the experimental and theoretical P3 LDOS is extended over the whole coupled system and is very similar to the electric field distribution of two M2 modes [Fig. 1(i)] each centered at one of the two D2 cavities forming the horizontal coupled system. Analogous results are obtained for P4 [Figs. 2(i) and 2(k)]. Therefore the large splitting of P3 and P4 resonances is attributed to their electromagnetic coupling, but still we have to consider that the two D2 cavities are not identical. Only by joining the information obtained for the two M1 and M2 modes of the D2 cavity that we can extract the coupling energy g. Indeed, from a statistical analysis of several single D2 cavities we have found that even if the absolute position of the M1 and M2 modes shifts up to 9 meV due to structural disorder, their energy separation varies only up to 1 meV. Therefore we can assume that the 2.6 meV energy splitting between P1 and P2 is also an estimation of the cavity detuning Δ for the two M2 modes. Therefore by using $\Omega = \sqrt{\Delta^2 + 4g^2}$ we obtain a coupling parameter $g = 5.9$ meV for
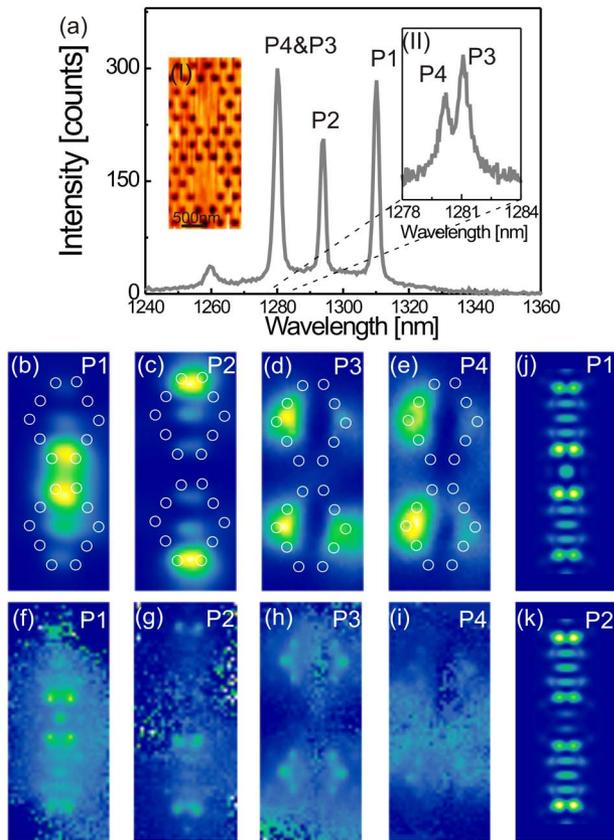
FIG. 3. (Color online) (a) Near-field spectrum of the vertically coupled D2 PC-MCs (averaged on a region of 1.5×3.5 μm^2). Inset (i): topographic map as obtained during the SNOM scan. Inset (ii): near-field high resolution spectrum that resolves the contributions of P3 and P4. [(b)–(e)] PL intensity maps associated to the peak P1-P4. [(f)–(i)] Spectral shift maps associated to peak P1-P4; in particular the maximum spectral shift in (f) and (g) is 0.15 nm, in (h) is 0.2 nm, and in (i) is 0.1 nm. [(j) and (k)] Calculated electric field distribution of P1 and P2 at 30 nm above the photonic membrane. All the maps have the same spatial extension (1.5×3.5 μm^2).

the M2 modes in the horizontal (along x) geometry.

In Fig. 3 the experimental results for vertically (along y) coupled PC-MCs are compared with the calculated electric field intensity. The PL maps indicate that P1 and P2 are delocalized over the entire system [Figs. 3(b) and 3(c)], and from the spectral shift maps [Figs. 3(f) and 3(g)], we attribute them to the two coupled-cavity modes originating from the M1 mode of a single D2 cavity with an overall photonic splitting $\Omega = 11.7$ meV. This attribution is clearly validated by the comparison of the experimental data [Fig. 3(f)] with the simulated map of the LDOS for P1, as reported in Fig. 3(j). The spatial distribution of both the experimental and theoretical LDOS is extended over the whole coupled system and is very similar to the electric field distribution of two M1 modes [Fig. 1(h)] each centered at one of the two D2 cavities forming the vertical coupled system. Similar results are obtained for P2 [Figs. 3(g) and 3(k)]. P3 and P4 show a very small splitting (0.8 meV), which, however, cannot be attributed to structural disorder. As demonstrated previously for P1 and P2 in the case of horizontally coupling, the fingerprint of frequency mismatch induced by disorder is the

localization of the LDOS over each single D2 cavity. The experimental near field maps of P3 and P4 [Figs. 3(d), 3(e), 3(h), and 3(i)] are instead extended over the whole coupled system, demonstrating that these two modes are the symmetric and the antisymmetric coupled-cavity modes originating from the M2 mode of the two single D2 cavities. Therefore, in this particular sample and following the argument discussed previously, the matching condition between the two independent D2 cavity modes is very well satisfied and the disorder induced detuning Δ is very small (much less than 0.8 meV). The experimental splittings for both P1-P2 and P3-P4 are therefore a direct measurement of the coupling energy g, which turns out to be $g = 5.9$ meV for the M1 mode and $g = 0.4$ meV for the M2 mode. Finally, numerical simulations of the coupled systems give a mode splitting in agreement with the experimental findings and the theoretical values are $g = 5.3$ meV ($g = 5.1$ meV) for the vertical (horizontal) alignment.

In summary, we addressed the photonic coupling of two closely spaced PC-MCs and by means of near field imaging, we demonstrated that it is possible to discriminate between the mode splitting due either to structural disorder or to mode coupling.

[1] A. D. Greentree, C. Tahan, J. H. Cole, and L. C. L. Hollenberg, Nat. Phys. **2**, 856 (2006).
[2] D. Englund, A. Faraon, B. Zhang, Y. Yamamoto, and J. Vučković, Opt. Express **15**, 5550 (2007).
[3] S. Ishii, A. Nakagawa, and T. Baba, IEEE J. Sel. Top. Quantum Electron. **12**, 71 (2006).
[4] M. Bayer, T. Gutbrod, J. P. Reithmaier, A. Forchel, T. L. Reinecke, P. A. Knipp, A. A. Dremin, and V. D. Kulakovskii, Phys. Rev. Lett. **81**, 2582 (1998).
[5] M. Ghulinyan, C. J. Oton, G. Bonetti, Z. Gaburro, and L. Pavesi, J. Appl. Phys. **93**, 9724 (2003).
[6] K. A. Atlasov, K. F. Karlsson, A. Rudra, B. Dwir, and E. Kapon, Opt. Express **16**, 16255 (2008).
[7] S. V. Zhukovsky, D. N. Chigrin, A. V. Lavrinenko, and J. Kroha, Phys. Rev. Lett. **99**, 073902 (2007).
[8] S. Mookherjea and A. Yariv, IEEE J. Sel. Top. Quantum Electron. **8**, 448 (2002).
[9] M. T. Hill, H. J. S. Dorren, T. De Vries, X. J. M. Leijtens, J. H. Den Besten, B. Smalbrugge, Y. S. Oel, H. Binsma, G. D. Khoe, and M. K. Smit, Nature (London) **432**, 206 (2004).
[10] N. Louvion, D. Gérard, J. Mouette, F. de Fornel, C. Seassal, X. Letartre, A. Rahmani, and S. Callard, Phys. Rev. Lett. **94**, 113907 (2005).
[11] P. Kramper, M. Kafesaki, C. M. Soukoulis, A. Birner, F. Müller, U. Gösele, R. B. Wehrspohn, J. Mlynek, and V. Sandoghdar, Opt. Lett. **29**, 174 (2004).
[12] S. I. Bozhevolnyi and L. Kuipers, Semicond. Sci. Technol. **21**, R1 (2006).
[13] S. Vignolini, F. Riboli, F. Intonti, M. Belotti, M. Gurioli, Y. Chen, M. Colocci, L. C. Andreani, and D. S. Wiersma, Phys. Rev. E **78**, 045603 (2008).
[14] F. Intonti, S. Vignolini, F. Riboli, A. Vinattieri, D. S. Wiersma, M. Colocci, L. Balet, C. Monat, C. Zinoni, L. H. Li, R. Houdré, M. Francardi, A. Gerardino, A. Fiore, and M. Gurioli, Phys. Rev. B **78**, 041401(R) (2008).
[15] M. Francardi, L. Balet, A. Gerardino, C. Monat, C. Zinoni, L. H. Li, B. Alloing, N. Le Thomas, R. Houdré, and A. Fiore, Phys. Status Solidi C **3**, 3693 (2006).